WATER RESOURCES RESEARCH, VOL. 43, W01401, doi:10.1029/2006WR005087, 2007

Effects of smoothing and regridding in numerical meander migration models

Alessandra Crosato[1]

Received 6 April 2006; revised 20 July 2006; accepted 6 September 2006; published 5 January 2007.

[1] Meander migration models include an as yet poorly investigated source of numerical errors related to the computation of the channel curvature, which are amplified by the procedure of adding and deleting grid points as the river planform evolves. The methods adopted to reduce these errors may influence size, form, and migration rate of the developing meanders, which creates uncertainties in the analysis of the results, limits the model applicability, and makes it necessary to treat the bank erodibility coefficients as calibration parameters. This becomes evident from a series of computational tests performed in order to compare two different methods of error reduction in the computed local channel curvature: cubic spline interpolations versus different levels of curvature smoothing. Since the problems discussed are common to most meander migration models, the tests performed were carried out for three models of different complexity. These were derived by applying different degrees of simplification to the basic equations for water flow and sediment motion of shallow curved channels.

Citation: Crosato, A. (2007), Effects of smoothing and regridding in numerical meander migration models, *Water Resour. Res.*, *43*, W01401, doi:10.1029/2006WR005087.

1. Introduction

[2] One-dimensional meander migration models are increasingly used, for river restoration projects [*Abad and García*, 2006] as well as for geological reconstructions [*Howard*, 1996]. They basically describe the location of the channel axis as a function of time, which entails a number of numerical complications. The quantification of migration rates requires the computation of the channel curvature, which needs to be estimated from the model result. As this procedure is susceptible to positive feedbacks in the computational errors, it has to be combined with an error reduction technique, e.g., a smoothing filter [*Crosato*, 1990; *Coulthard and Van De Wiel*, 2006]. Moreover, as the river planform develops, the channel length tends to change, to the extent that it may be necessary to introduce or remove points from the computational grid [*Crosato*, 1990; *Sun et al.*, 1996; *Lanzoni et al.*, 2005]. This increases the errors related to the computation of the local channel curvature and makes a smoothing filter inevitable. The effects of smoothing filters on the computed planform evolution have hardly been investigated, so far.

[3] This work aims at exploring these effects by comparing the results of some computational tests in which different filters are used. In meander models the computation of the local channel centerline curvature has a prominent role, because the computed local erosion rates are always, directly and indirectly, dependent on that. The computed value of the local curvature depends on the alignment of the points describing the channel centerline. A small local deviation from a smooth centerline is seen by the models as a small-scale (spurious) channel bend, which tends to grow in time. Spurious bends always show up during long-term computations, because introducing or removing grid points always implies a small local deviation from a perfectly smooth centerline. A numerical filter is therefore needed to smooth out the spurious channel bends which originate from an imperfect alignment of the grid points. However, introducing such a filter has consequences for the channel alignment and for the computation of centerline curvature and erosion rates.

[4] The computational tests performed aimed at simulating the long-term evolution of a series of meanders, starting from an (almost) straight channel, with the objective of quantifying the effects of using different filters on the short- and long-term planimetric evolution and on the erosion rates. Distinct methods were investigated: cubic spline interpolations and different levels of ''curvature smoothing''. In order to generalize the reasoning, three meander models of different complexity were used in the tests. They were derived from the mathematical model of *Crosato* [1987, 1989] by applying different degrees of simplification, and solved using the numerical code MIANDRAS [*Crosato*, 1990].

[5] The results show that the choice of the method affects to a great extent the shape and the migration rates of meanders, although they should depend on the physical model only. Therefore numerical aspects cannot be overlooked when analyzing the results of meander models. Another important consequence is that, in order to reproduce the planform changes of real rivers, the erodibility coefficients cannot be determined a priori as a function of the local bank characteristics, but must be

[1]Section of Hydraulic Engineering, Delft University of Technology, Delft, Netherlands.

0043-1397/07/2006WR005087$09.00

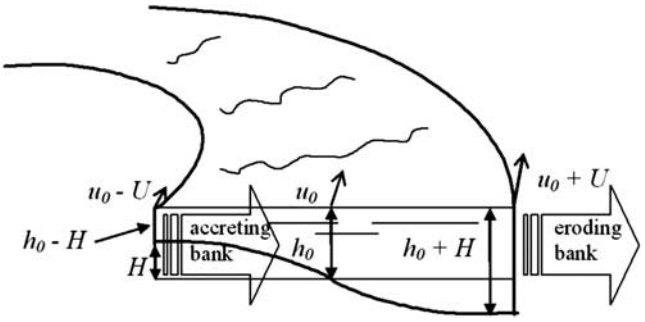

Figure 1. Transverse variations of flow velocity and water depth in a curved channel as assumed in the model. Legend: u_0 and h_0, cross-sectionally averaged velocity and water depth; U and H, near-bank excess of velocity and water depth (near the outer bank the excesses are positive; near the inner bank excesses are negative).

calibrated on historical migration rates. The erodibility coefficients act in fact as bulk parameters, since they incorporate many physical and numerical aspects that influence the erosion rates.

2. Model Description

[6] Meander models compute the planform evolution of meandering rivers. In order to do so, at every computational time step they determine the lateral shift of the river, which results from the local bank erosion and accretion rates. A common assumption is that the river width remains constant, which is achieved by assuming that the bank accretion rate at one side of the channel equals the bank erosion rate at the opposite side. The simplest (kinematic) models relate bank erosion to the channel centerline curvature with a phase lag to account for the downstream migration of the meanders [*Ferguson*, 1984; *Howard*, 1984]. Dynamic models include descriptions for the flow in the rivers, usually in linearized form. Since the model of *Ikeda et al.* [1981], many meander models assume that bank erosion is proportional to the local near-bank excess flow velocity. This can be regarded as a linearization of *Osman and Thorne*'s [1988] process of parallel bank retreat with a Krone-Partheniades formulation for bank erosion [*Mosselman*, 1992].

[7] The model of *Ikeda et al.* [1981], as well as the more recent model of *Abad and García* [2006], obtains the phase lag between curvature and bank erosion from the momentum and continuity equations of water, leading to a term accounting for the longitudinal adaptation of the near-bank excess flow velocity. The models of, among others, *Crosato* [1987], *Johannesson and Parker* [1989], *Howard* [1992], *Sun et al.* [1996], and *Zolezzi and Seminara* [2001] include also the longitudinal adaptation of the water depth, which is obtained by coupling the momentum and continuity equations for the water motion with a sediment transport formula and a sediment balance equation. In this way models are able to reproduce the formation of steady alternate bars inside the river channel, which influences the near-bank excess flow velocity and bank erosion. Some of these models are compared and discussed by *Camporeale et al.* [2005].

[8] The mathematical model of *Crosato* [1987, 1989] computes the longitudinal profiles of the near-bank excesses of flow velocity and water depth above the cross-sectionally averaged values, named U and H, respectively (Figure 1). These excesses are caused by the local channel curvature and by upstream flow disturbances, such as a change of the centerline curvature. The local bank erosion rate is assumed to be a function of U and H. The excess velocity, U, accounts for the effects of fluvial erosion, which is driven by the local flow velocity [*Ikeda et al.*, 1981]. The excess water depth, H, accounts for geomechanical instability, which is based on the consideration that bank instability increases in case of toe erosion (higher near-bank water depth) [*Crosato*, 1989]. With this type of formulation, the cross-sectionally averaged values of velocity and water depth, u_0 and h_0, become the threshold values below which banks do not erode but accrete. The transverse profiles of water depth and velocity are assumed to be perfectly point symmetrical with respect to the channel centerline (point bar–pool configuration, Figure 1), which implies that the bank accretion rate equals the bank erosion rate at the opposite side and that the river width remains constant.

[9] The basic equations are obtained from the steady state 2-D depth-averaged continuity and momentum equations for water in shallow channel bends [*Kalkwijk and De Vriend*, 1980], which, in order to simulate the interaction between water and sediment, are coupled to a sediment transport formula and to a sediment balance equation. The effect of the outer bend superelevation of the water free surface is retained in the momentum equations, but neglected with respect to water depth in the continuity equation (assuming a mildly curved channel). The equations are linearized and, assuming that the timescale of the meander development is much larger than the timescale of the transverse channel bed adaptation, the temporal term in the sediment balance equation is neglected. The implication is that the model is not able to take into account the migrating bars that form in channels with a low sinuosity [*Tubino and Seminara*, 1990]. Another assumption is that the timescale of the meander development is much smaller than the timescale of the longitudinal bed slope adaptation. The river bed slope is updated at every time step by dividing the valley slope (considered as a constant and independent parameter) by the river sinuosity.

[10] Upon linearization of the momentum and mass balance equations for small U and H with respect to u_0 and h_0 the equation for the near-bank velocity excess becomes [*Crosato*, 1989]:

$$\frac{\partial U}{\partial s} + \frac{U}{\lambda_W} = \left(\frac{1}{2\lambda_W}\frac{u_0}{h_0}\right)H - \frac{u_0}{k_B}\frac{\partial \Gamma}{\partial s} - \frac{(2-\sigma)}{2\lambda_W}\frac{u_0}{k_B}\Gamma \qquad (1)$$

where s is the downstream coordinate; h_0 and u_0 are the cross-sectionally averaged values of water depth and velocity, respectively; λ_W is the flow adaptation length, given by $\lambda_W = \frac{C^2 h_0}{2g}$, in which C is the coefficient of Chézy and g is the acceleration due to gravity; $k_B = \frac{m\pi}{B}$ is the wave number of the velocity and water depth perturbations assumed sinusoidal in transverse direction (the near-bank values of these perturbations are the near-bank excesses U and H, Figure 1), with B being the river width and m the number of branches inside the channel (for meandering

rivers $m = 1$, for braided rivers $m > 1$); Γ is the curvature term, given by $\Gamma = \frac{1}{R_C}(\frac{m\pi}{2})$, in which R_c is the local radius of curvature of the channel centerline. The coefficient σ has been added to the transverse bed friction term in order to reproduce the effects of the secondary flow momentum convection, not previously included in the model, σ is used as a calibration coefficient and has value between 0 and 2.

[11] The equation for the water depth excess is derived from the sediment transport and sediment balance equations [*Crosato*, 1989]:

$$\frac{\partial H}{\partial s} + \frac{H}{\lambda_S} = \frac{h_0}{u_0}(b-1)\frac{\partial U}{\partial s} + Ah_0^2 k_B \Gamma \tag{2}$$

where λ_S is the bed adaptation length, given by $\lambda_s = \frac{1}{(m\pi)^2} h_0(\frac{B}{h_0})^2 f(\theta_0)$, in which $f(\theta_0) = \frac{0.85}{E}\sqrt{\theta_0}$ is an empirical relation taking into account the effects of the transverse bed slope [*Talmon et al.*, 1995], with E being a calibration coefficient and θ_0 the Shields parameter. In the equation b is the degree of non linearity in the dependence of sediment transport on the flow velocity, defined as $b = \frac{u_0}{S_0}\frac{dS_0}{du_0}$, with S_0 being the cross-sectionally averaged value of sediment transport per unit of channel width (b is equal to the exponent in case of a power law dependence: $S_0 \propto u_0^b$). A is the coefficient accounting for the effects of the curvature-induced spiral flow on the bed shear stress direction, given by the relation: $A = \frac{2\alpha_1}{\kappa^2}(1 - \frac{\sqrt{g}}{\kappa C})$ [*Olesen*, 1987], where κ is the von Kármán constant and α_1 is a calibration coefficient.

[12] The equation for the lateral shift of the channel axis reads [*Crosato*, 1989]:

$$\frac{\partial n}{\partial t} = E_u U + E_h H \tag{3}$$

where n denotes the transverse coordinate, t is time and E_u and E_h are the so-called "erodibility coefficients".

[13] Equations (1) and (2) give rise to a second-order differential equation, which can be expressed either in the variable H or U. The equations in H or U are identical in the homogeneous part, whereas they are different in the source terms. The equation in H reads as follows:

$$\begin{aligned}&\frac{\partial^2 H}{\partial s^2} + \left[\frac{1}{\lambda_S} - \frac{(b-3)}{2\lambda_W}\right]\frac{\partial H}{\partial s} + \frac{H}{\lambda_S \lambda_W} \\ &= -\frac{h_0}{k_B}(b-1)\frac{\partial^2 \Gamma}{\partial s^2} + \frac{h_0}{k_B}\left[Ah_0 k_B^2 - \frac{(2-\sigma)(b-1)}{2\lambda_W}\right] \\ &\quad \cdot \frac{\partial \Gamma}{\partial s} + \frac{h_0}{k_B}\left(\frac{Ah_0 k_B^2}{\lambda_W}\right)\Gamma\end{aligned} \tag{4}$$

[14] Depending on the value of the factor in brackets in the second term, the solution of the homogeneous part of the equations is either harmonic or purely exponential. The harmonic solution represents the overshoot [*Struiksma et al.*, 1985] or overdeepening phenomenon [*Parker and Johannesson*, 1989] and corresponds to a channel bed with non propagating alternate bars [*Seminara and Tubino*, 1989]. It has the following form:

$$H(s) = H(0)\exp\left[-\frac{s}{L_D}\right]\sin\left[\frac{2\pi}{L_P}(s + s_P)\right] \tag{5}$$

where $H(0)$ is the near-bank water depth excess at the upstream boundary (caused by a flow disturbance, such as a change of curvature); $H(s)$ is the near-bank water depth excess at the distance s from the upstream boundary (measured along the channel centerline); s_P is the spatial lag; $2\pi/L_P$ and $1/L_D$ are the wave number and damping coefficient, respectively.

[15] The wave number and the damping coefficient follow from substitution of equation (5) into the homogenous version of equation (4):

$$\frac{2\pi}{L_P} = \frac{1}{2\lambda_W}\left[(b+1)\frac{\lambda_W}{\lambda_S} - \left(\frac{\lambda_W}{\lambda_S}\right)^2 - \frac{(b-3)^2}{4}\right]^{1/2} \tag{6}$$

$$\frac{1}{L_D} = \frac{1}{2\lambda_W}\left[\frac{\lambda_W}{\lambda_S} - \frac{(b-3)}{2}\right] \tag{7}$$

[16] If the damping coefficient, $1/L_D$, is large, nonpropagating alternate bars are strongly damped and vanish within a short distance downstream.

[17] For infinitely long bends with fully developed flow the longitudinal gradients of water depth and flow velocity vanish. Equations (1) and (2) become

$$\frac{U}{\lambda_W} = \left(\frac{1}{2\lambda_W}\frac{u_0}{h_0}\right)H - \frac{(2-\sigma)}{2\lambda_W}\frac{u_0}{k_B}\Gamma \tag{8}$$

$$\frac{H}{\lambda_S} = Ah_0^2 k_B \Gamma \tag{9}$$

and the near-bank excesses U and H become simply proportional to the local curvature (represented by Γ).

[18] A model based on equations (8) and (9) for the near-bank flow and water depth excesses and on equation (3) for the lateral shift of the channel axis is equivalent to a no-lag kinematic model, because at every point the bank erosion rate is proportional to the local curvature. In this case meanders only grow in size, without migrating.

[19] If the relaxation effect is included in the flow velocity equation, but not in the equation for the water depth, the model becomes similar to the one developed by *Ikeda et al.* [1981]. This is achieved by describing the flow and water depth excesses with equations (1) and (9). The maximum value of the flow velocity occurs downstream of the maximum curvature, which causes meanders to grow in size and to migrate downstream.

[20] All models including the relaxation effect in both flow velocity and water depth equations, such as the model of Crosato (based on equations (1) and (2)), simulate meanders that grow in size and contemporarily migrate both in downstream and upstream direction. The latter depends on the position of alternate bars inside the channel [*Crosato*, 1990].

3. Problem Definition

[21] In MIANDRAS, and in meander models in general, a major source of numerical errors lies in the computation of the channel centerline curvature that needs to be repeated at every time step. There are several ways to compute the curvature at point J; the simplest one is to compute the

Table 1. Flume Conditions[a]

	Value
Valley slope	0.003
Channel width, m	0.60
Discharge, m^3/s	0.685×10^{-2}
D_{50} sediment, μm	216
D_{50} sediment, μm	271
Chézy, $m^{1/2}/s$	21.6

[a]Experiment by *Struiksma and Crosato* [1989].

radius of curvature of the circle passing though the three points J − 1, J and J + 1. A vector product can then be used to assess the sign of the curvature, which indicates whether the channel is turning to the right or to the left (this is important to identify the inner and the outer bank in a river bend). Unfortunately, this method is weak if the three points are almost on a straight line, which occurs when the curvature is very small, and if the points are very close to one another. This can lead to two types of numerical errors; one has to do with the value of the curvature, the other with its sign. The second type of error is the most dangerous. A mistake in the sign of curvature immediately leads to a positive feedback, thus to a growing error (instability).

[22] Reducing the time step of the computations is not effective in decreasing this type of error. Instead, it is necessary to introduce a numerical filter that is able to select developing bends based on their spatial scale and to remove the spurious small-scale bends generated by local inaccuracies. One simple method, here called ''curvature smoothing'' [*Crosato*, 1990; *Coulthard and Van De Wiel*, 2006], averages the value of the curvature at point J with the curvatures of preceding and following points. There are many possible functions to be used; a simple one, which is the one adopted by *Crosato* [1990] in the computational model MIANDRAS, is the following weighted average:

$$\Gamma_J = \frac{\Gamma_{J-1} + 2\Gamma_J + \Gamma_{J+1}}{4} \tag{10}$$

where $\Gamma_J = \frac{1}{R_{CJ}} (\frac{m\pi}{2})$ and R_{CJ} is the radius of curvature of the circle passing through the three points $J - 1$, J and $J + 1$. With equation (10) (averaging) the curvature at point J depends on the five points: $J - 2$, $J - 1$, J, $J + 1$ and $J + 2$. This averaging, here referred to as ''curvature smoothing'', can be repeated several times, which results in including more and more points in the computation of the curvature. This method smooths out small-scale bends, depending on the number of points involved. The direct effect of applying this method is the reduction of the curvature variations along s, with consequent damping of the maximum values. Indirect effects are the general lowering of the water depth and velocity excesses, leading to a reduction of the bank erosion rates.

[23] Other methods to smooth out small-scale spurious bends are based on curve fitting. The curvature at point J can be computed as the curvature of the best fitting circle considering 5, 7, or more points, using, for instance, the least squares method. Instead of a circle, one can also use a parabola or another curve. Again, the number of grid points taken into account selects the scale of the bends to be removed. *Sun et al.* [1996] and *Lanzoni et al.* [2005] used cubic spline interpolations, which is another way of smoothing out small-scale bends. Spline interpolations [*Duris*, 1977] include a parameter for varying the smoothness of the fit, which can be used as an indirect way to select the scale of the small-scale bends to be smoothed out. The implication of applying this method is that the curve describing the channel planform is altered, which implies that the spline interpolation requires some sort of optimization.

[24] The position of the grid points is not constant during the numerical simulations. In general, the distance between grid points increases as a meander grows, but it can also happen that grid points approach each other, for instance when due to meander migration at a certain location a bend disappears. With increased distances between successive grid points, the channel centerline looses smoothness and appears more and more like a series of circle segments. Besides, the larger the distance the lower the model resolution and the more inaccurate the numerical procedure is. With decreased distances between successive grid points, the curve through a number of successive grid points can be confused (by the program) with a straight line, which increases the susceptibility to numerical errors. These problems introduce the necessity of inserting new grid points when the distance between two successive grid points has become too large and of deleting grid points when the distance has become too small [*Crosato*, 1990; *Sun et al.*, 1996]. Unfortunately, the procedure of inserting grid points can also be the origin of new small-scale spurious bends. It is practically impossible to insert the new grid point exactly on the channel centerline, without any small errors in its coordinates. The method to improve the accuracy of the computations can thus become the source of new computational errors. In practice, the procedure of inserting and deleting grid points makes the use of smoothing filters inevitable.

4. Methods

[25] With the objective of quantifying the effects of different smoothing filters on the shape and size of developing meanders and on the erosion rates, several numerical tests were carried out using the program MIANDRAS. The tests regarded the two types of smoothing filters that can be distinguished in previous works: curvature smoothing [*Crosato*, 1990; *Coulthard and Van De Wiel*, 2006] and cubic spline interpolations [*Sun et al.*, 1996; *Lanzoni et al.*, 2005]. Curvature smoothing was

Table 2. Model Choices

	Value
Sediment transport	
Formula	E-H[a]
b	5
Calibration coefficients	
α_1 (equation (2))	0.50
σ (equation (1))	2.00
E (equation (2))	0.50
Erodibility coefficients	
E_u (equation (3))	0.116×10^{-5}
E_h, 1/s (equation (3))	0.00
Time step, days	4

[a]*Engelund and Hansen* [1967].

Table 3. Initial Conditions

	Value
Initial sinusoidal planimetry	
Sinuosity	1.00
Length, m	6.00
Amplitude, m	0.01
h_0, m	0.045
u_0, m/s	0.25
θ_0	0.38
λ_S, m	0.84
λ_W, m	1.08
L_P, m	6.04
$1/L_D$, 1/m	0.129

applied at two different levels: applying equation (10) once (local curvature based on 5 points) and applying equation (10) four times (local curvature based on 11 points). Computational tests also included a run without filters, in which the channel centerline curvature was computed from the circle passing through 3 points (the current grid point plus the proceeding and following points).

[26] Three different mathematical models were tested, all based on the same equation for the lateral channel shift (equation (3)): (1) a generic no-lag kinematic model (near-bank flow and water depth excesses derived from equations (8) and (9)), (2) an Ikeda-type model (near-bank flow and water depth excesses derived from equations (1) and (9)), and (3) the model of Crosato (near-bank flow and water depth excesses derived from equations (1) and (4), which are based on equations (1) and (2)).

[27] The computational tests used the values of channel width, discharge, valley slope and sediment characteristics of the straight flume experiment carried out by Struiksma and *Crosato* [1989], summarized in Table 1, but with an initial centerline alignment given by a low-amplitude sinusoid. Several preliminary runs were carried out in order to optimize a number of parameters (listed in Table 2), as well as the minimum and maximum distances between successive grid points, based on which the model inserts and deletes grid points. The step size used for the discrete cubic spline coincided with the maximum distance between grid points. Spline interpolation was also optimized by comparing the channel centerline alignments before and after interpolation. This optimization regarded the amount of smoothing in comparison to data fitting, which is weighted by the parameter ρ. Small values of ρ enhance the smoothness of the approximation, whereas large values of ρ improve the fitting of the points [*Duris*, 1977]. On the basis of the results of the preliminary runs ρ was given a value of 20.

[28] Apart from the preliminary runs, the numerical tests performed to quantify the effects of the numerical filters for the different models had the same initial conditions, coefficients, time step, minimum and maximum distances between grid points and ρ (only for spline interpolations). The bank erodibility was assumed spatially uniform. The initial conditions are listed in Table 3. The numerical tests are summarized in Table 4.

[29] The model of *Ikeda et al.* [1981], as well as several other meander models [e.g., *Johannesson and Parker*, 1989; *Howard*, 1992; *Sun et al.*, 1996], does not include a formulation for the geotechnical component of the bank migration rate. For this reason in the computational tests the erosion rate was only related to the near-bank velocity excess ($E_h = 0$). In the model of Crosato the longitudinal variation of near-bank water depth and velocity excesses can be described by two damped sinusoids having the same wavelength, but with a phase lag (equation (5)). The maximum value of U occurs more downstream than the maximum value of H. Taking into account also the geotechnical component of the bank migration rate would systematically move the position of the maximum erosion rate more upstream, but would not change the conclusions of the analysis. The occurrence of cutoffs was not taken into account, implying that meanders may cross each other in their final development stages.

5. Results

[30] The results of the preliminary runs showed that the optimal distance between successive grid points had the order of half the channel width. More in general, the distance had to be larger than approximately one third of the channel width and smaller than the channel width. The basis of this rule is merely empirical. The computational results showed that when the distance between successive grid points was less than approximately one third of the channel width, the model became more susceptible to numerical errors, with as implication the growth of spurious small-scale bends. When the distance between successive grid points was larger than one channel width the model results became unacceptably inaccurate.

[31] The results of the numerical tests showed that the effects of using a different method to smooth out small-scale bends were the strongest for the no-lag kinematic model, which, due to its immediate response to the local curvature, is the most susceptible to instability (Table 4). In this case, without filter the program stopped almost immediately. Spline interpolations yielded a jumbled channel alignment, which was comparable to the alignment obtained when smoothing the curvature once (curvature based on five

Table 4. Numerical Tests Performed

Model	Number of Time Steps	No Filter	Curvature Smoothing 5 Grid Points	Curvature Smoothing 11 Grid Points	Spline Interpolation
No-lag kinematic	250	program stops almost immediately	program stops after 190 time steps (760 days)	normal end	normal end
Ikeda type	250	normal end	normal end	normal end	normal end
Ikeda type	1000	normal end	normal end	normal end	normal end
Crosato	250	normal end	normal end	normal end	normal end

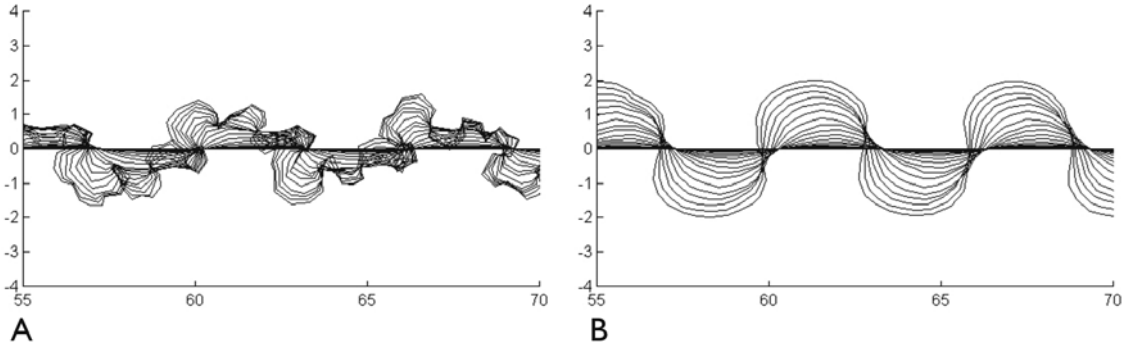

Figure 2. No-lag kinematic model. Meander development is after 760 days. Output is every 40 days, and distances are in meters. (a) Curvature smoothing once (curvature based on 5 grid points), program terminated after 190 time steps (760 days). (b) Curvature smoothing four times (curvature based on 11 grid points).

points, Figure 2a). Curvature smoothing repeated four times gave a smoother alignment. With 11 grid points all small-scale bends were smoothed out, but the channel centerline was still a bit irregular (Figure 2b). Since the erosion rates in the kinematic model are directly proportional to the local curvature, meanders grew but did not migrate.

[32] The Ikeda-type model and the model of Crosato remained stable also without using a numerical filter (Table 4), but in general this does not always occur, because it depends on the set of parameters used. With the same setup the Ikeda-type model and the model of Crosato result in different migration rates. In order to obtain meanders in a similar development stage, the runs with the Ikeda-type model had to be 4 times longer (covering 4000 days instead of 1000).

[33] The results of the Ikeda-type model are shown in Figure 3a (using curvature smoothing once) and 3b (using spline interpolations). With this model the different numerical filters resulted in meanders with similar shape, but different development stages. This indicates that for the Ikeda-type model the numerical filter used mainly influences the speed of meander growth. In a reach far from the upstream and downstream boundaries, the averaged maximum migration rate without smoothing filter was 0.388×10^{-3} m/d, with curvature smoothing (curvature based on five points) 0.341×10^{-3} m/d and with the optimized cubic spline interpolation 0.475×10^{-3} m/d. The differences can be attributed to the filter used because all parameters had identical values in all computational tests.

[34] The results of computational tests performed with the model of Crosato (summarized in Table 4) are shown in Figures 4a (using curvature smoothing once) and 4b (using spline interpolations). This time, after the same number of time steps meanders not only have different sizes, but also different shapes: those obtained with curvature smoothing once (Figure 4a) have a shape similar to the meanders obtained with the Ikeda-type model (Figures 3a and 3b), whereas those obtained using the cubic spline interpolation (Figure 4b) are more distorted. Far from the upstream and downstream boundaries, the average maximum migration rate without smoothing filter was 1.70×10^{-3} m/d, with curvature smoothing once 1.65×10^{-3} m/d; and with the optimized cubic spline interpolation 1.58×10^{-3} m/d. The conclusion is that the numerical filter can affect both growth rate and shape of developing meanders.

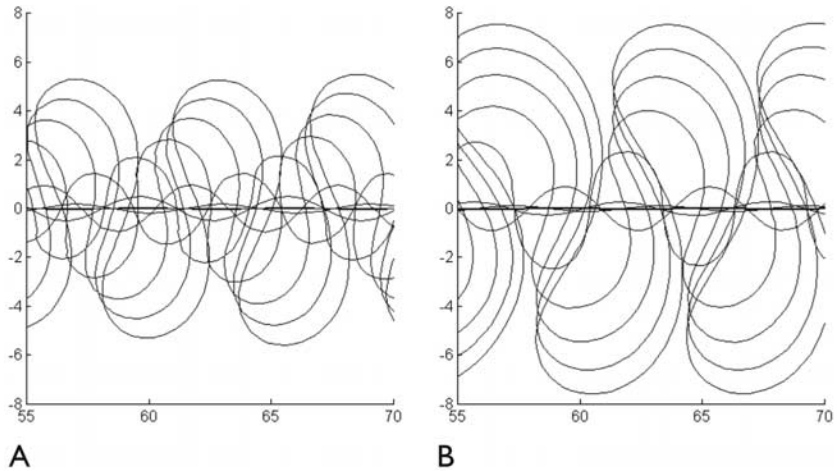

Figure 3. Ikeda-type model. Meander development and channel migration are after 4000 days. Output is every 400 days, and distances are in meters. (a) Curvature smoothing once (curvature based on 5 grid points). (b) Cubic spline interpolation.

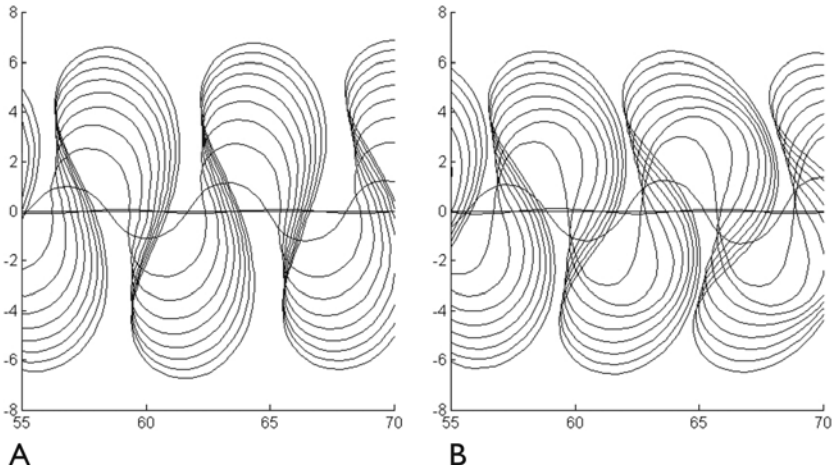

Figure 4. Crosato's model. Meander development and channel migration are after 1000 days. Output every is 100 days, and distances are in meters. (a) Curvature smoothing once (curvature based on 5 grid points). (b) Cubic spline interpolation.

[35] The channel centerline alignments obtained with different numerical filters (Crosato's model) at different stages of meander development are compared in Figure 5. Comparing size and form of the meanders obtained with the different numerical filters after the same number of time steps allows observing that with the increasing of the computational time the differences in meander amplitude reduce, whereas the differences related to the form of the meanders increase. In practice, this means that for long-term predictions the uncertainties related to the meander amplitude that are due to the numerical filters tend to reduce, but

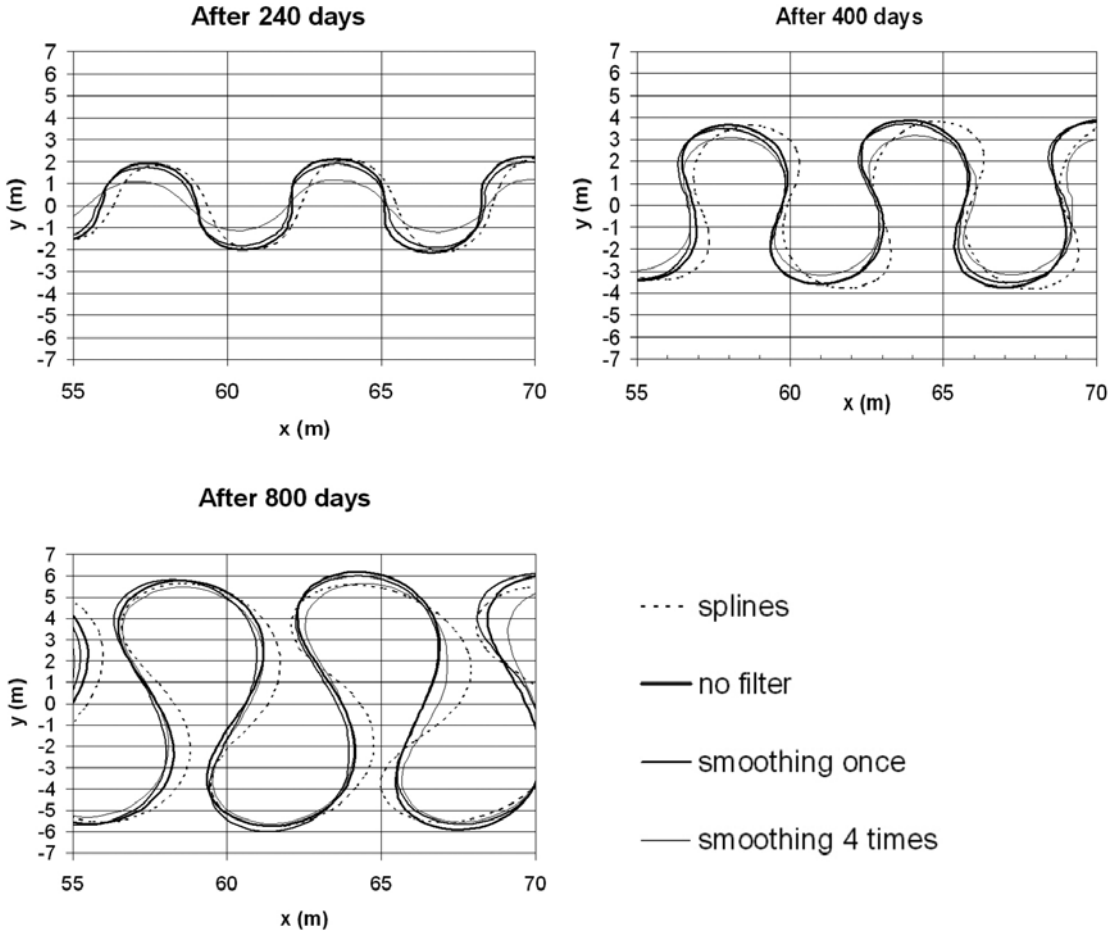

Figure 5. Channel centerline alignments obtained with Crosato's model using different filters.

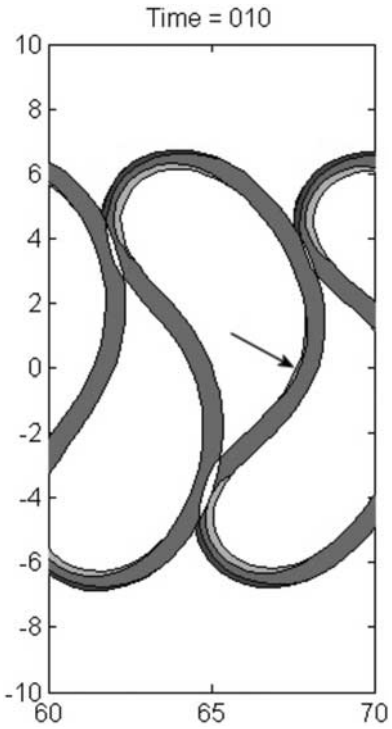

Figure 6. Detail of the final bed topography after 1000 days with Crosato's model using cubic spline interpolations. Distances are in meters. A slight midmeander point bar is observable (arrow).

the uncertainties related to the form of meanders tend to increase.

6. Discussion and Conclusions

[36] The foregoing has shown that meander migration models have a particular source of numerical errors that has received little attention, so far. This source is related to the necessity of using numerical filters to reduce the errors related to the computation of the local channel curvature. The numerical tests with three conceptually different meander models showed that size, form and migration rates of meanders depend on the numerical filter used.

[37] The no-lag kinematic model resulted stable only when applying curvature smoothing four times. The Ikeda-type model [*Ikeda et al.*, 1981; *Abad and García*, 2006] was the least affected by the choice of the filter, which seemed to influence only the growth rate of meanders, but not the shape. The same dependence can be expected for kinematic models with a space lag [*Ferguson*, 1984; *Howard*, 1984] and for other meander models that, although based on different approaches, can be classified as belonging to this category, such as the models of *Lancaster and Bras* [2002] and the cellular model of *Coulthard and Van De Wiel* [2006]. Instead, the model of *Crosato* [1987] was affected by the smoothing filter in both growth rate and shape of meanders. This model behaves like the one of *Ikeda et al.* [1981] when the damping coefficient $1/L_D$ (equation (7)) is large, but when this is small there is a strong dependence on the upstream curvature changes. The same likely applies also to the other meander models capable of reproducing the overdeepening phenomenon [*Johannesson and Parker*, 1989; *Howard*, 1992; *Sun et al.*, 1996]. The conclusion is that model output should be analyzed by taking into account all uncertainties, not only those related to the physical simplifications in the governing equations and to the values of the parameters used but also the uncertainties related to the numerical aspects.

[38] Non propagating alternate bars can be observed in real rivers, where they influence bank erosion and channel migration. The model reproduction of these bars (overdeepening) and of their effects on bank erosion should therefore be as accurate as possible. Unfortunately, error-reducing numerical filters can influence this because the removal of small-scale bends, by reducing the longitudinal curvature variations, can also imply the suppression of nonpropagating alternate bars in their early stage. In the present computational tests, the formation of point bars in midmeanders only occurred when using the spline interpolation (Figure 6). As these bars did not form in the computation without smoothing filters (Figure 7), one might argue that the spline interpolation introduces realistic-looking but, in fact, unrealistic effects. However, which one is the method that gives the most realistic results? The answer can only be given by reproducing formation and growth of large meanders from a straight channel in laboratory. For this type of experiments the approaches of *Smith* [1998] (using cohesive soil) and of *Gran and Paola* [2001] (with riparian vegetation) appear the most promising.

[39] The computational tests performed do not represent real situations (input based on data from a flume experiment and uniform bank erodibility). Moreover, they simulate the planimetric evolution of an initially almost straight channel

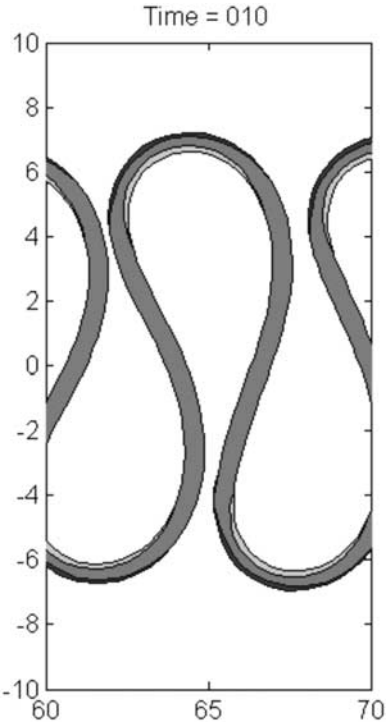

Figure 7. Detail of the final bed topography after 1000 days with Crosato's model without using a smoothing filter (curvature based on 3 grid points). Distances are in meters.

during a relatively long time interval, which for a real river may correspond to several centuries. For shorter simulations and real rivers the choice of the smoothing procedure can be expected to produce a higher impact on the erosion speed than on the shape of the meanders.

[40] The difference in erosion speed between models and smoothing filters is remarkable. This implies that for real rivers it is not possible to determine the erodibility coefficients a priori, based on bank properties, presence of vegetation, etc., and creates the necessity of always calibrating the erodibility coefficients on field observations, historical maps, aerial photographs and remote-sensing imagery. When using this type of models the physical bank characteristics can only explain a part of the differences between the erodibility coefficients at different points. In practice, the erodibility coefficients act as bulk parameters that encompass many schematization effects. This means that, for the time being, these models require non physical calibration of the erodibility coefficients in order to comply with reality.

[41] The most recent management approaches [*Silva et al.*, 2004] are based on the idea that rivers need some vital space to accomplish their functions, which introduced the concept of "river corridor" or "streamway" with the slogan: "freedom space to the river" [*Malavoi et al.*, 2002]. The river corridor is an artificially maintained, regularly flooded, alluvial belt where the river is allowed to erode its banks, in a controlled "natural" state. Uncontrolled bank erosion could take away valuable land and for this reason the knowledge of bank erosion processes, meander evolution and cutoffs is of essential importance for the design of such corridors [*Piégay et al.*, 2005]. The width of the river corridor is determined by the meander amplitude and by the occurrence of cutoffs, which is in turn governed by the form of the meanders. For what numerical aspects concerns the model of *Crosato* [1987] appeared more suitable for long-term predictions of the amplitude rather than form of meanders. Therefore when used to predict cutoffs the model should be appropriately calibrated on previous occurrences.

Notation

A coefficient, dimensionless.
b degree of nonlinearity of sediment transport on the flow velocity, dimensionless.
B river width, m.
C Chézy coefficient, $m^{1/2}/s$.
E calibration coefficient, dimensionless.
E_h erodibility coefficient (geomechanical instability), 1/s.
E_u erodibility coefficient (fluvial erosion), dimensionless.
g acceleration due to gravity, m/s^2.
H near-bank water depth perturbation (near-bank excess with respect to h_0), m.
h_0 cross-sectionally averaged water depth, m.
k_B transverse wave number of velocity and water depth perturbations, 1/m.
L_D longitudinal damping length, m.
L_P longitudinal wavelength of flow and water depth perturbation, m.
m number denoting the transverse perturbation mode or number, dimensionless.
n transverse coordinate, m.
R_c radius of curvature of the channel centerline, m.
s downstream coordinate, m.
s_P spatial lag, m.
t time, s.
U near-bank velocity perturbation (near-bank excess with respect to u_0), m/s.
u_0 cross-sectionally averaged velocity, m/s.
α_1 calibration coefficient, dimensionless.
Γ curvature term, 1/m.
θ_0 Shields parameter, dimensionless.
κ von Kármán constant, dimensionless.
λ_S bed adaptation length, m.
λ_W flow adaptation length, m.
σ calibration coefficient, dimensionless.

[42] **Acknowledgments.** This research is granted by the Water Research Centre Delft. The author wishes to thank Huib de Vriend, Marco Toffolon, and Erik Mosselman for their valuable comments.

References

Abad, J. D., and M. H. García (2006), RVR Meander: A toolbox for re-meandering of channelized streams, *Comput. Geosci.*, *32*, 92–101.

Camporeale, C., P. Perona, A. Porporato, and L. Ridolfi (2005), On the long-term behaviour of meandering rivers, *Water Resour. Res.*, *41*, W12403, doi:10.1029/2005WR004109.

Crosato, A. (1987), Simulation model of meandering processes of rivers, in *Extended Abstracts of International Conference Euromech 215 Mechanics of Sediment Transport in Fluvial and Marine Environments*, pp. 158–161, Univ. of Genoa, Genoa, Italy.

Crosato, A. (1989), Meander migration prediction, *Excerpta*, *4*, 169–198.

Crosato, A. (1990), Simulation of meandering river processes, *Commun. Hydraul. Geotech. Eng. Rep. 90-3*, 104 pp., Delft Univ. of Technol., Delft, Netherlands.

Coulthard, T. J., and M. J. Van De Wiel (2006), A cellular model of river meandering, *Earth Surf. Processes Landforms*, *31*, 123–132, doi:10.1002/esp.1315.

Duris, C. S. (1977), Discrete interpolation and smoothing spline functions, *SIAM J. Numer. Anal.*, *14*, 686–698.

Engelund, F., and E. Hansen (1967), *A Monograph on Sediment Transport in Alluvial Streams*, Dan. Tech. Press, Copenhagen.

Ferguson, R. I. (1984), Kinematic model of meander migration, in *River Meandering*, *Proceedings of Rivers '83*, edited by C. M. Elliott, pp. 942–951, Am. Soc. of Civ. Eng., Reston, Va.

Gran, K., and C. Paola (2001), Riparian vegetation controls on braided stream dynamics, *Water Resour. Res.*, *37*(12), 3275–3283.

Howard, A. D. (1984), Simulation model of meandering, in *River Meandering, Proceedings of Rivers '83*, edited by C. M. Elliott, pp. 952–963, Am. Soc. of Civ. Eng., Reston, Va.

Howard, A. D. (1992), Modeling channel migration and floodplain sedimentation in meandering streams, in *Lowland Floodplain Rivers: Geomorphological Perspectives*, edited by P. A. Carling and G. E. Petts, pp. 1–41, John Wiley, Hoboken, N. J.

Howard, A. D. (1996), Modelling channel evolution and floodplain morphology, in *Floodplain Processes*, edited by M. G. Anderson, D. E. Walling and P. D. Bates, pp. 15–62, John Wiley, Hoboken, N. J.

Ikeda, S., G. Parker, and K. Sawai (1981), Bend theory of river meanders. Part 1. Linear development, *J. Fluid Mech.*, *112*, 363–377.

Johannesson, H., and G. Parker (1989), Linear theory of river meanders, in *River Meandering*, *Water Res. Monogr. Ser.*, vol. 12, edited by S. Ikeda and G. Parker, pp. 181–214, AGU, Washington, D. C.

Kalkwijk, J. P. T., and H. J. De Vriend (1980), Computation of the flow in shallow river bends, *J. Hydraul. Res.*, *18*(4), 327–342.

Lancaster, S. T., and R. L. Bras (2002), A simple model of river meandering and its comparison to natural channels, *Hydrol. Processes*, *16*, 1–26, doi:10.1002/hyp.273.

Lanzoni, S., B. Federici, and G. Seminara (2005), On the convective nature of bend instability, in *River, Coastal and Estuarine Morphodynamics: RCEM 2005*, edited by G. Parker and M. H. Garcia, pp. 719–724, Taylor and Francis, Philadelphia, Pa.

Malavoi, J.-R., J.-N. Gautier, and J.-P. Bravard (2002), Free space for rivers: A geodynamical concept for sustainable management of the water

resources, in *River Flow 2002*, edited by D. Bousmar and Y. Zech, pp. 507–514, A. A. Balkema, Brookfield, Vt.

Mosselman, E. (1992), Mathematical modelling of morphological processes in rivers with erodible cohesive banks, *Commun. Hydraul. Geotech. Eng. Rep. 92-3*, 134 pp., Delft Univ. of Technol., Delft, Netherlands.

Olesen, K. W. (1987), Bed topography in shallow river bends, *Commun. Hydraul. Geotech. Eng. Rep. 87-1*, Delft Univ. of Technol., Netherlands.

Osman, A. M., and C. R. Thorne (1988), Riverbank stability analysis I: Theory, *J. Hydraul. Eng.*, *114*(2), 143–150.

Parker, G., and H. Johannesson (1989), Observations on several recent theories of resonance and overdeepening in meandering channels, in *River Meandering*, *Water Resour. Monogr. Ser.*, vol. 12, edited by S. Ikeda and G. Parker, pp. 379–415, AGU, Washington, D. C.

Piégay, H., S. E. Darby, E. Mosselman, and N. Surian (2005), A review of techniques available for delimiting the erodible river corridor: A sustainable approach to managing bank erosion, *River Res. Appl.*, *21*, 1–17, doi:10.1002/rra.881.

Seminara, G., and M. Tubino (1989), Alternate bar and meandering: Free, forced and mixed interactions, in *River Meandering*, *Water Resour. Monogr. Ser.*, vol. 12, edited by S. Ikeda and G. Parker, pp. 267–320, AGU, Washington, D. C.

Silva, W., J. P. M. Dijkman, and D. P. Loucks (2004), Flood management options for the Netherlands, *Int. J. River Basin Manage.*, *2*(2), 101–112.

Smith, C. E. (1998), Modeling high sinuosity meanders in a small flume, *Geomorphology*, *25*, 19–30.

Struiksma, N., and A. Crosato (1989), Analysis of a 2-D bed topography model for rivers, in *River Meandering*, *Water Resour. Monogr. Ser.*, vol. 12, edited by S. Ikeda and G. Parker, pp. 153–180, AGU, Washington, D. C.

Struiksma, N., K. W. Olesen, C. Flokstra, and H. J. De Vriend (1985), Bed deformation in curved alluvial channels, *J. Hydraul. Res.*, *23*(1), 57–79.

Sun, T., P. Meaking, T. Jossang, and K. Schwarz (1996), A simulation model for meandering rivers, *Water Resour. Res.*, *32*, 2937–2954.

Talmon, A. M., N. Struiksma, and M. C. L. M. Van Mierlo (1995), Laboratory measurements of the direction of sediment transport on transverse alluvial-bed slopes, *J. Hydraul. Res.*, *33*(4), 495–517.

Tubino, M., and G. Seminara (1990), Free-forced interactions in developing meanders and suppression of free bars, *J. Fluid Mech.*, *214*, 131–159.

Zolezzi, G., and G. Seminara (2001), Downstream and upstream influence in river meandering. Part 1. General theory and application to overdeepening, *J. Fluid Mech.*, *438*, 183–211.

A. Crosato, Section of Hydraulic Engineering, Delft University of Technology, Stevinweg 1, NL-2628 CNDelft, Netherlands. (a.crosato@tudelft.nl)